

## XPS-SIMS Study on the Surface Chemistry of Commercially Available Activated Carbons Used as Catalyst Supports

P. ALBERS, K. DELLER, B. M. DESPEYROUX, A. SCHÄFER, AND K. SEIBOLD

*Degussa AG, Rodenbacher Chaussee 4, P.O. Box 13 45, D-6450 Hanau 1, Germany*

Received March 1, 1990; revised June 27, 1991

The specific surface properties of activated carbons used as support materials for precious metal catalysts were investigated by XPS and SIMS. The surface C/O ratios and changes in the spectrum of surface-functional groups after different chemical pretreatments were measured. A correlation between the differences in graphitic/aromatic and aliphatic carbon contributions and of hydrogen present on the carbonaceous surfaces and the corresponding XPS and SIMS signals has been observed. The influence of natural impurities of activated carbons on the catalytic activity of powdered-type catalysts and the effect of surface carbides on the precious metal dispersion on pelletized shell-type catalysts are presented. The information gives a better understanding of the interdependence between the surface chemistry of the activated carbon and the performance of the catalysts. © 1992 Academic Press, Inc.

### 1. INTRODUCTION

Surface characterization of finely divided catalyst-support materials is important for a better understanding of the interactions between precious metal solutions and supports in the various stages of impregnation processes, and can lead to the improvement and control of catalyst preparation techniques.

Activated carbon is widely used for the preparation of powdered and fixed-bed catalysts. As with all natural materials, variations in morphology and surface chemistry can tremendously affect the final properties of the prepared catalysts. In the present study X-ray photoelectron spectroscopy (XPS) and secondary ion mass spectrometry (SIMS) results on the characteristic features present in the topmost atomic layers of the carbon support are presented.

XPS and SIMS cannot stand alone in judging the quality and applicability of any actual activated support: simultaneous use of scanning and transmission electron microscopy (SEM, TEM), energy-dispersive analysis of X-rays (EDX), X-ray fluorescence (XRF),

and surface area measurements are needed. However, they can help to fingerprint specific surface conditions in the complex process of tailoring a catalyst.

### 2. ACTIVATED CARBON AS SUPPORT FOR PRECIOUS METAL HETEROGENEOUS CATALYSTS

Activated carbons acting as supports for precious metals must possess adequate physical properties, including morphology, form, size, bulk density, porosity, pore size distribution, and specific surface area, to be of use in a catalyst for a chemical process. Especially the interaction between the active phase and the surface of the support is of particular importance for the catalyst activity and the product selectivity of the overall catalytic process.

Powdered, granulated, or formed, pelletized carbons are used as supports, originating from natural sources such as beechtree, oak, and pine wood, peat, lignite, anthracite, as well as coconut shell. The activation of these raw materials is carried out by two different processes, namely steam/gas activation or chemical activation

( $\text{ZnCl}_2$ ,  $\text{H}_3\text{PO}_4$ ,  $\text{HCl}$ , or other acid treatments).

By elution/leaching or physical/mechanical removal of oxygen-enriched surface areas and of other impurities or by chemical decomposition or oxidative modification of the carbon surface, a suitable surface polarity for the interaction between the carbon surface and precious metal solutions can be obtained.

An important contribution to the catalytic activity of activated carbon and to the redox processes in precious metal impregnation is most likely given by the ratio between graphitic/aliphatic carbon and the different classes of surface functional groups (1–4). The latter are usually characterized as follows:

(a) "acidic surface oxides," such as carboxylic, phenolic, carbonyl-type groups, and lactic hydroxyl groups,

(b) "basic surface oxides," such as organic nitrogen-containing compounds and quinoid groups.

Normally, the acidic oxides dominate the overall surface chemistry of activated carbon, leading to hydrophilic properties. If, furthermore, alkaline or alkaline-earth salts of these surface oxides are present, the hydrophilic behavior of the carbon surface is enhanced significantly. At a certain concentration level of, for example, alkaline-earth salts, the adsorption capability for organic compounds and therefore the catalytic conversion may decrease remarkably.

XPS and SIMS allow the detection of these surface functional groups and specific surface contaminations even at comparatively low concentrations.

### 3. EXPERIMENTAL

#### 3.1 Measurements

The XPS measurements were conducted using a Leybold EA11/100 energy analyzer and a double anode X-ray source ( $\text{MgK}\alpha$ ,  $\text{AlK}\alpha$ ) at a power of 100–150 W.

Spectra were recorded in the  $\Delta E = \text{const.}$  mode, pass energy 50 and 75 eV. All the

spectra presented in this paper and plotted together for comparison were taken under identical conditions. The base pressure of the spectrometer was  $2 \times 10^{-10}$  mbar (ending with Ti sublimation pumps and  $\text{N}_2$  cryostage) and in the  $10^{-9}$  mbar range during the measurements.

A sample was introduced using a separate, differentially pumped desorption stage, controlled by mass spectrometers. Afterward, the sample was transferred into the spectrometer chamber under ultrahigh vacuum conditions. Therefore, surface states that are stable under vacuum conditions are characterized after desorption of the highly volatile surface species adsorbed on these carbon support materials.

For spectrometer calibration (5), the Au  $4f_{7/2}$  (83.9 eV) and the Cu  $2p_{3/2}$  (932.5 eV) signals were repeatedly recorded. The area analyzed was  $1.5 \text{ cm}^2$  to provide reasonable statistics in probing a representative area of each sample. This was done in the analysis of carbon powders as well as for pellets.

The SIMS spectra were recorded using a Leybold IQ 12/38 ion gun at primary beam energies between 1 and 5 kV and at primary currents of 1–3  $\mu\text{A}$  of  $\text{Ar}^+$ . The secondary ions were collected in a Balzers QMG 511 quadrupole mass spectrometer with a Leybold ion-optical system.

For data acquisition and evaluation, an HP 1000 computer and DS100 data set (Leybold) were utilized. Quantitative evaluations were based upon reference measurements on standard targets and on relative sensitivity factors for the actual XPS analyzer. Data refinement was performed by Sawitzky/Golay algorithms and curve fitting was performed by Gauss/Lorentz routines, referenced against organic and inorganic carbonaceous materials and to the numerous data, published on polymer systems (6, 7).

#### 3.2 Sample Charging

Falsification of the peak shapes and positions due to differential charging of the carbon surfaces was ruled out by additional measurements with and without standard

TABLE I  
Selection of Some Typical Concentration Values of Carbon and Oxygen on  
Different Carbon Surfaces

	Material	C	O
I	Carbon for spectroscopic purposes (Ringsdorff)	98.6	1.4
	Carbon black (Degussa)	99.2	0.8
	Carbon black (Degussa), oxidized	90.1	9.9
	Graphite, powdered (Alfa Products)	96.6	3.4
	Graphite, foil (Alfa Products)	99.8	0.2
II	Reproducibility check		
	Activated carbon, powdered		
	Beech tree, HCl-treated		
	First measurement	90.8	9.2
	Second measurement	90.9	9.1
IIIa	Activated carbon, pine wood		
	Powdered, raw material	76.9	23.1
	Powdered, HCl-treated (1 M)	83.5	16.5
	Powdered, HNO <sub>3</sub> -treated (1 M)	88.8	11.2
	Powdered, HNO <sub>3</sub> -treated (2 M)	87.7	12.3
IIIb	Activated carbon, pine wood		
	Same type as IIIa, different lot		
	Powdered, raw material	79.0	21.0
	Powdered, HCl-treated (1 M)	85.2	14.8
	Powdered, HNO <sub>3</sub> -treated (1 M)	92.1	7.9
IV	Activated carbon, different sources		
	Bitumen	93.1	6.9
	Peat	93.2	6.8
	Coconut	93.1	6.9
	Coconut (modified)	94.1	5.7
V	Activated carbon, pellets, exhibiting surface carbides		
	"As delivered"	93.1	6.9
	After mechanical removal of surface carbides	97.1	2.9

Note. The data represent the ratio of the areas of C and O in the topmost atomic layers.

neutralization techniques, using a low-energy electron flood gun as well as surface biasing of the sample holders and variation of the electrostatic potential of the entrance aperture of the energy analyzer.

The information depth of XPS is slightly greater in the case of carbonaceous materials than in the case of metal oxides or metals and is most likely dependent on the degree of surface graphitization. The mean free path for electrons in carbon was given in Refs. (8, 9) to be in the range of 1.5–1.7 nm (for inelastic scattering). Therefore, signal contributions

from deeper layers can be a reason for asymmetric peak broadening as an unavoidable source of error in peak fitting processes, even if electrostatic charging of the surfaces analyzed is compensated. The XPS data should not therefore be discussed as absolute, quantitative values, but the comparison of observations on similar carbon surfaces can certainly reveal significant differences.

### 3.3 Vacuum Requirements

Usually activated carbons for technical applications show very high BET surface

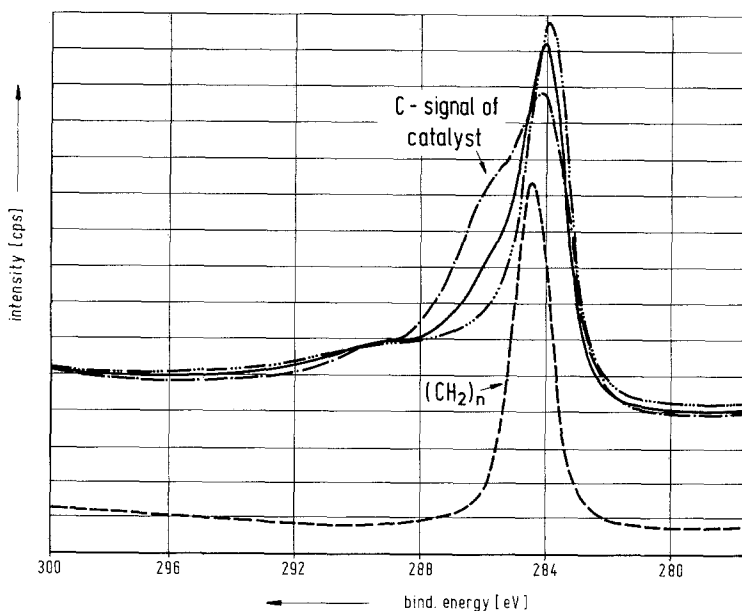


FIG. 1. Comparison of the C 1s XPS signals of a thin layer of  $(\text{CH}_2)_n$  on a gold support and three different activated carbon supports (pine wood) after Pt impregnation; line broadening at higher binding energies due to different contributions of C/O compounds.

areas of about  $1000 \text{ m}^2 \text{ g}^{-1}$ . Therefore, it is essential, and is confirmed by our experiments, that the determination of a specific surface chemistry by XPS and SIMS be carried out under precisely defined vacuum conditions checked by mass spectrometric residual gas analysis.

We ensured that the measurements presented are not disturbed by residual gas effects since the activated carbon itself could act as a getter material and that the XPS signals of carbon and oxygen did not show alterations during data accumulation by re-deposition of gaseous compounds or by radiation-induced effects.

#### 4. RESULTS AND DISCUSSIONS

##### 4.1 Carbon/Oxygen Ratio on Different Carbon Surfaces

In Table 1, a selection of some typical C/O concentration values on different carbon surfaces is given, derived from XPS measurements by using relative sensitivity factors. The values represent the ratio of the areas of C and O in the topmost atomic layers.

Table 1, part I gives the C and O values

of carbon black, graphite, and carbon for spectroscopic applications. In Table 1, II–V, the corresponding results on activated carbon are presented. The reproducibility of the measurements shown in part II, as well as the comparison between parts IIIa and IIIb, seems to be quite encouraging.

The effects of acid activation ( $\text{HCl}$ ,  $\text{HNO}_3$ ), demonstrated in Table 1, parts IIIa and IIIb, show a general decrease of the surface oxide content, as well as the start of a slight oxidizing effect caused by the change in  $\text{HNO}_3$  concentration from 1 to 2  $M$ . The C/O results on materials originating from different natural resources (bitumen, peat, coconut) in Table 1, part IV are not adequate to allow a discrimination based only on this C/O surface ratio of significant differences in the surface chemistry. The values in Table 1, part V, are discussed in Section 4.5.2.

##### 4.2 Line Shape Analysis of the C 1s Photoelectron Spectroscopy Signals

In Fig. 1 the carbon 1s XPS signal is shown. The signal of a very thin layer of

TABLE 2

The Binding Energy Positions of the C 1s XPS Signals for Different Compounds (Typical Reference Values; Own Measurements and Literature Values (5, 6); in Electron Volts, eV)

Carbides	280–283.5
Graphitic carbon	284.0–284.5
(CH <sub>2</sub> ) <sub>n</sub>	284.6 (5)
Primary alcohols	285.3–286.1
Ether	286–287
Ester/carbonates	288–290 <sup>a</sup>
Carbonates	289–290
C/(EL) <sub>n</sub>	>290 <sup>b</sup>

<sup>a</sup> On carbon surfaces, lactones and quinoid groups are usually detected (1, 3) with binding energies in this region.

<sup>b</sup> EL = electronegative elements like F. Around 291–294 eV the plasmon/shake-up satellite of graphitic/aromatic carbon can be found as additional proof for the degree of surface graphitization. This signal is only detected on predominantly graphitic/aromatic surfaces. The shake-up satellite is caused by III\* transitions in aromatic regions, activated by the C 1s photoelectron.

synthetic wax on high-purity gold is compared qualitatively with the C 1s signals of some activated carbon supports in the final preparation state of precious metal catalysts.

The signal of the carbon film is very narrow and symmetrical, representing nearly exclusively one single species of carbon, whereas the corresponding signals of the catalyst specimens are formed by changing contributions of different surface compounds, which can be separated and identified by curve fitting and subsequent referencing to binding energies of known compounds. A typical compilation of binding energies for C/O functional groups and different chemical states of carbon is given in Table 2.

In Figures 2 and 3 results of line shape analysis by Gauss/Lorentz fitting procedures are compared. The signals indicate that on commercially available carbon materials for catalyst support purposes a very broad variety of totally different compounds can be found, detectable by characteristic chemical shifts on the binding energy scale of the C 1s signal.

The C 1s signal is shifted in an energy interval, extending from about 281/283 eV (carbide carbon, Fig. 2, IV; Fig. 3, III, IV) up to 293 eV (C/F compounds, Fig. 3, I).

It has been confirmed that no charging effects could disturb these results.

It is a remarkable feature that even if the C/O ratio does not suggest the presence of any effects (Table 1, IV, V) the XPS signals show pronounced differences in the surface chemistry of the activated carbons (Fig. 2, IV; Fig. 3, I, II, IV).

#### 4.3 Surface Alterations by Selective Conditioning Processes

In Fig. 2, parts II and III, the C 1s signals of a beech tree-activated carbon surface before and after treatment with 1 M HNO<sub>3</sub> are compared. The signal maxima are shifted on the binding energy scale, because oxidic and aliphatic surface species are partly removed from the carbon surface. After acid treatment, the surface contributions of graphitic and aromatic carbon dominate.

Carbonates, lactones, and other higher oxidized surface compounds are almost absent, as could be discerned from the corresponding binding energy-values of the line shape analysis. The use of higher concentrated HNO<sub>3</sub> (2 M and more), on the other hand, leads to an oxidation of significant amounts of C–OH and carbonyl functions, similar to the quantitative changes measured for the C/O ratio after treatment of pine wood supports with 1 or 2 M HNO<sub>3</sub> (Table 1, IIIa and IIIb). As an overall effect, the increase of aromatic/graphitic surface carbon was again observed. General trends in alteration of the surface chemistry of activated carbons by chemical pretreatment are shown in Table 3.

The acid treatment of raw activated carbon samples under usual conditions (dilute acids) leads to lower surface concentrations of oxidized carbon compounds, especially carbonates, lactones, and esters, and aromatic compounds of probably lower mass numbers are partly removed from the top-

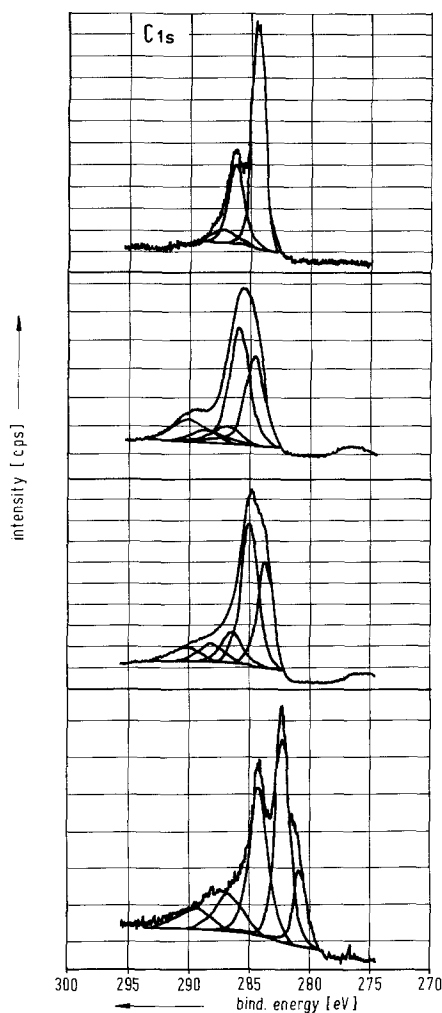


FIG. 2. Activated carbon, C 1s XPS signal. (I) Graphitized carbon surface, containing additional C=O functions (pine wood, after steam activation). (II) Raw material, powder (beech tree); n.b. lactones and carbonates present at binding energies between 288 and 290 eV; no graphitic/aromatic carbon present. (III) As II after HNO<sub>3</sub> (1 M) treatment; reduced signal intensities of higher oxidized C/O compounds; graphitic/aromatic carbon detectable at 284.4 eV. (IV) Pine wood, pellets, after HCl (1 M) treatment; n.b. surface carbides present.

most atomic layers. In general, signal contributions from species in the aromatic and graphitic state increase. After acid treatment, higher amounts of pure aliphatic carbon (C 1s signal around 284.6–285.2 eV) were no longer detected, neither on powdered nor on pelletized specimens.

After precious metal impregnation, the C 1s signal maximum is again often shifted further to lower binding energies. In Fig. 1 it can be seen that the C 1s maxima are located around 284.0 eV indicating a dominating contribution of aromatic/graphitic carbon, but on these surfaces C/O functional groups are still significantly resolved by XPS.

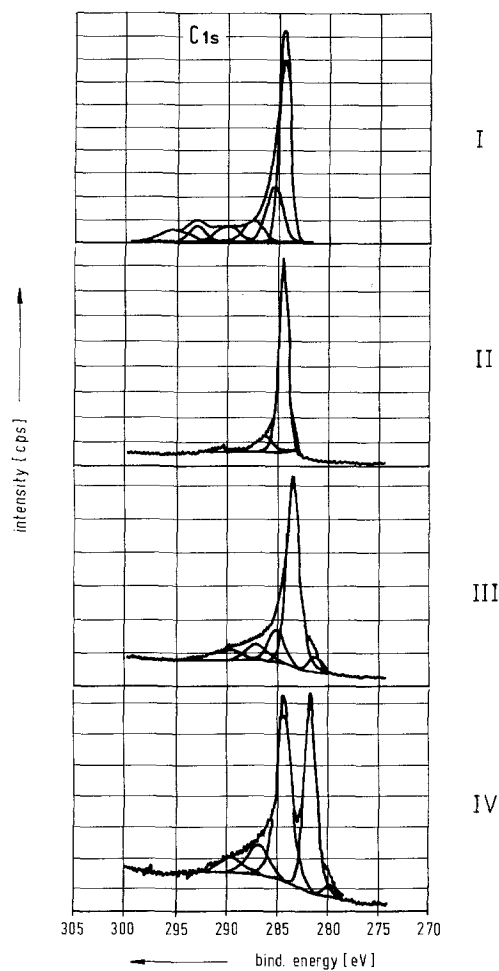


FIG. 3. Activated carbon, C 1s XPS signal. (I) Raw material, coconut; n.b. C/F compounds around 293 eV, surface concentration of fluorine about 4% (XPS). (II) Raw material, bitumen; aromatic/graphitic carbon, binding energy of peak maximum: 284.4 eV. (III) Pellets, pine wood, after HNO<sub>3</sub> (1 M) treatment; binding energy of peak maximum: 284.2 eV. (IV) Pellets, pine wood, after HCl (1 M) treatment (other origin as III); surface carbides present.

TABLE 3  
Influences of Some Technical Pretreatment Processes  
on Activated Carbon Surfaces

Pretreatment	Trends (XPS results)
HCl (1 M), dilute HNO <sub>3</sub> (1 M) HCl/HNO <sub>3</sub> , dilute mixture	Reduced total oxygen and aliphatic C concentrations, increase of graphitic/aromatic carbon signals
HNO <sub>3</sub> (2 M) and higher conc.	Oxidation of OH- and carbonyl functions, slightly enhanced oxygen concentration, compared to the effects of dilute acids
NaOCl	Slightly enhanced oxygen concentrations compared to HCl- treatment, increase of C-OH group concentrations
NaHCO <sub>3</sub>	Reduced total oxygen concentrations, increase of C-OH surface groups

Note. Typical features determined by XPS.

#### 4.4 Combined XPS/SIMS Results

The relative intensities of the SIMS signals C<sup>-</sup> and C<sub>2</sub><sup>-</sup> in correlation with the binding energy values of the maximum of the XPS C 1s signal and small but significant contributions of the III\* shake-up signal (Table 2) can be a good qualitative measure for the amounts of aromatic/graphitic surface states.

The positively charged fragment ions such as CH<sup>+</sup>, CH<sub>2</sub><sup>+</sup>, and CH<sub>3</sub><sup>+</sup> can indicate the presence of higher amounts of aliphatic surface compounds. The signals CH<sup>-</sup> and C<sub>2</sub>H<sup>-</sup> are a good measure for the hydrogen chemically bound in partially hydrided or hydrogen-enriched surface regions.

In Fig. 4 a correlation between the position of the C 1s XPS signal and different SIMS fragment ion intensities, normalized to the actual BET surface of each sample, is shown. Points 1 and 2 are results on graphite (Table 1), and 3-11 are results obtained on activated carbon in the raw and acid-treated surface state. With increasing C<sub>2</sub><sup>-</sup> SIMS intensity, the XPS signal is shifted to lower binding energies (284.0 eV), indicat-

ing dominating amounts of graphitic/aromatic carbon.

The comparison of untreated (10, 11) and acid-treated (3, 5, 6) surfaces shows that not only oxidic compounds (Table 1, III) but also aliphatic compounds that are not volatile under the ultrahigh vacuum conditions of the XPS/SIMS spectrometer are partially removed by acid treatment. This interpretation is confirmed by the systematic changes of the CH<sub>x</sub><sup>+</sup> and C<sub>2</sub>H<sup>-</sup> SIMS intensities.

In Fig. 5 the XPS-results on surface oxygen (Table 1) are compared with the C<sub>2</sub><sup>-</sup>/C<sub>2</sub>H<sup>-</sup> ratio determined with SIMS before and after acid treatment. Again, a systematic decrease of surface oxygen (XPS) and surface hydrogen (SIMS) can be observed. The changes due to treatment with more concentrated HNO<sub>3</sub> suggest that the graphitic/aromatic surface regions are beginning to be degraded; furthermore, C/H compounds are detected by the variation of the C<sub>2</sub><sup>-</sup>/C<sub>2</sub>H<sup>-</sup> ratio.

In Fig. 6 the C and O SIMS signals are compared for pine wood in the raw (6, I) and HCl-treated (6, II) condition. The decrease of the oxygen concentration measured with

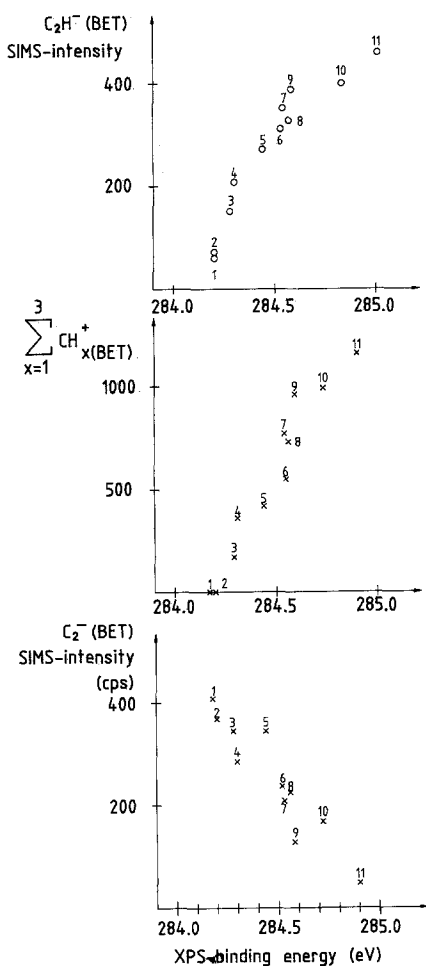


FIG. 4. Correlation between XPS and SIMS results on carbonaceous materials. XPS, binding energies of the maxima of the C 1s signals; SIMS,  $C_2^-$  fragment ions as a measure for aromatic/graphitic carbon;  $\sum_{x=1}^3 CH_x^+$  fragment ions as a measure for aliphatic surface contributions.  $C_2H^-$  fragment ions as a measure for surface hydrogen, predominantly in aromatic regions. SIMS values normalized on BET surface areas. 1, graphite, foil; 2, graphite, powdered; 3, pine wood, HCl-treated; 4, bitumen, raw; 5, pine wood,  $HNO_3$ -treated; 6, pine wood,  $HNO_3$ -treated; 7, peat, raw; 9, beech tree, raw; 10, pine wood, raw; 11, pine wood, raw.

XPS (Table 1, IIIa, IIIb) is confirmed by these typical SIMS results.

#### 4.5 Influence of Surface Impurities

Very often, activity problems of fresh prepared precious metal catalysts are not

caused by external contaminants from the catalyst preparation process or by incomplete reduction of the precious metal component to the suitable valency state but by impurities of the support material itself, which are responsible for selective blocking effects. These impurities are often enriched in the surface layers of the carbonaceous supports. This can be demonstrated by XPS and SIMS.

**4.5.1 Influence of surface impurities on the activity of powdered activated carbon catalysts.** In Figs. 7 and 8 the deactivating influence of excessive amounts of Ca and Fe on the activity of a freshly prepared powdered palladium/carbon catalyst is shown. The catalyst performance in the cinnamic acid hydrogenation standard test is plotted against the corresponding Ca and Fe concentrations of the specimens. Raising the Ca and Fe concentrations of the support leads to a tremendous decrease of hydrogenation activity of the catalyst. Comparison of RFA and XPS results have shown that Ca and Fe are present on the surface as well as in the bulk material.

**4.5.2 Influence of surface carbides of pelletized activated carbons.** On the surfaces of pelletized carbonaceous supports, sometimes significant concentrations of carbidic carbon contributions to the actual integral C 1s signal can be detected, as shown in Fig. 2, part IV or in Fig. 3, part III and IV (signals around 280–283 eV were measured).

The chemical shifts observed indicate that carbides of Ca, Fe, and other elements are present. This has an adverse effect on impregnation, especially that of shell-type precious metal catalysts.

In Table 4 quantitative examples for the correlation between the surface carbide concentration on pelletized activated carbon before precious metal impregnation and parameters of the prepared Pd/C catalysts are compared. Supports A and D are of similar origin, while supports B and C were prepared by mechanical abrasion treatment of support A. In Table 1, part C the alterations of the C/O values due to the abrasion pro-



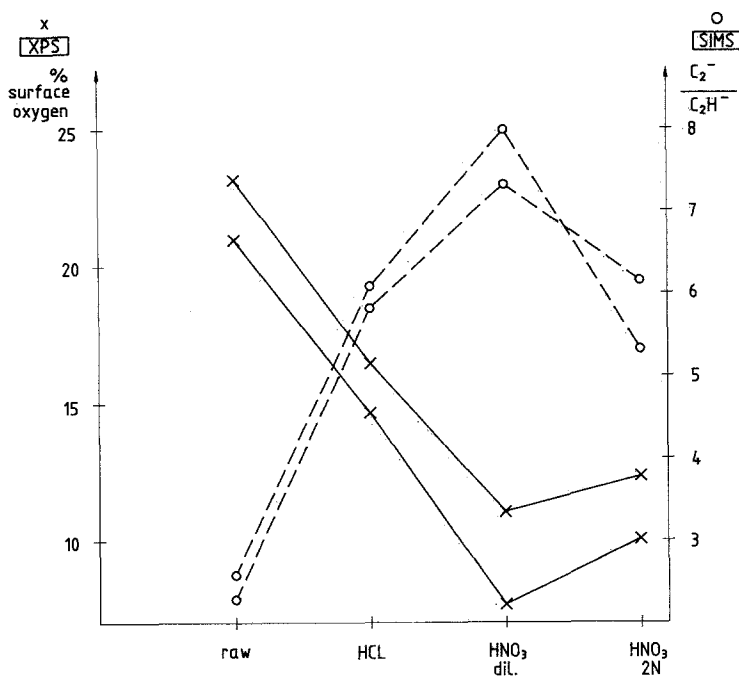


FIG. 5. Correlation between XPS and SIMS data. XPS: Percentage of surface oxygen for two different charges of pine wood after different pretreatments (X). SIMS:  $C_2^-/C_2H^-$  ratio of these samples (O).

cess are noted. The CO adsorption data (Table 4) show that on the mostly carbidic surfaces a poor Pd dispersion is obtained. Catalysts prepared by the use of support D without any carbidic contaminations show

the best performance in hydrogenation processes.

In Fig. 9 (I-III), the changes of the  $Ca^+$  SIMS signal as a function of sputter time are shown. This indicates that Ca is predomi-

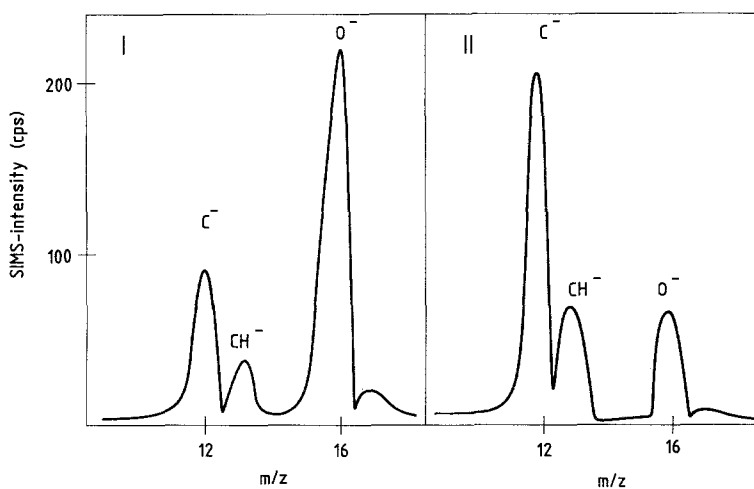


FIG. 6. SIMS fragment ion intensities of pine wood (I, raw; II, after HCl treatment).

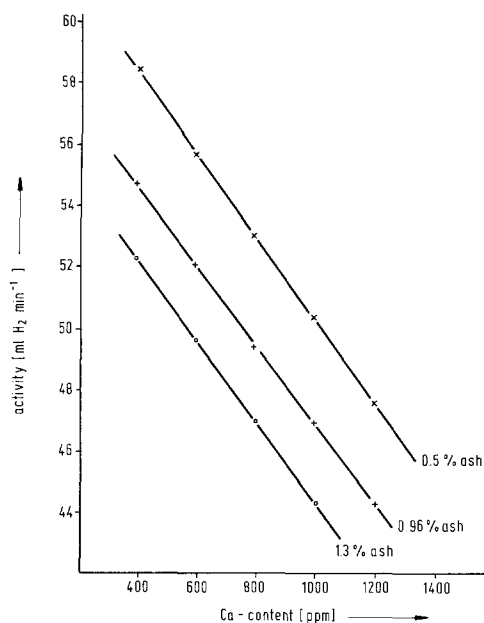
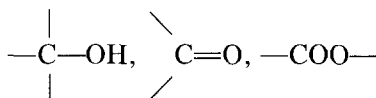


FIG. 7. Correlation between Ca content of Pt/C catalysts and activity in the hydrogenation of cinnamic acid; Ca content determined by RFA (10). Reaction conditions: pressure, 10 mbar; temperature,  $25 \pm 0.2^\circ\text{C}$ ; stirrer rate, 2,000 rpm (stirrer with sparger unit); amount catalyst, 230 mg; amount cinnamic acid, 10 g; ethanol (absolute), 120 g.

nantly enriched on the outer perimeter of the pellets and that the pellet production process must be optimized.

From Table 4 it can be derived that the Pd dispersion increases with increasing content of C/O functional groups



and aromatic/graphitic surface area but decreases with the amount of carbidic carbon.

In the considered catalytic process, high CO adsorption values of the prepared catalysts proved to be mostly adequate. Comparison of the results on supports A and D demonstrates that for the catalyst performance differences in the BET values or pellet porosity are of minor importance.

In Fig. 10 SIMS fragment ion intensities for samples A and D (Table 4) before Pd impregnation are compared. It can be distinguished qualitatively that on D higher amounts of surface hydrogen that together with C–OH and carbonyl-groups may be of additional positive influence in the redox processes of the catalyst impregnation are present. The corresponding C 1s XPS sig-

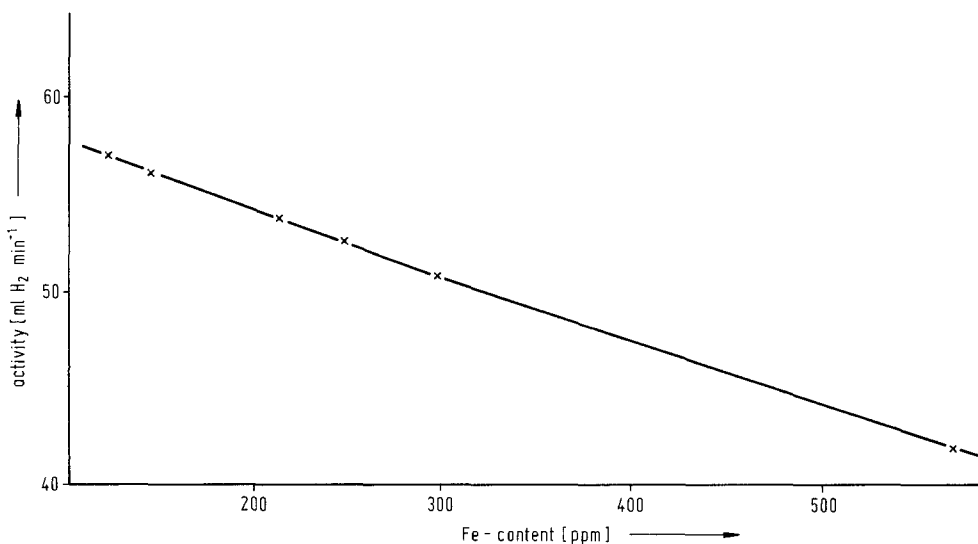


FIG. 8. Correlation between Fe content of Pt/C catalysts and activity in the hydrogenation of cinnamic acid; Fe content determined by RFA (10). Reaction conditions: pressure, 10 mbar; temperature  $25 \pm 0.2^\circ\text{C}$ ; stirrer rate, 2,000 rpm (stirrer with sparger units); amount catalyst, 230 mg; amount cinnamic acid, 10 g; ethanol (absolute), 120 g.

TABLE 4  
Influence of the Surface Concentrations of Different Chemical States of Carbon  
for Different Lots of Activated Carbon Pellets

	Support A	Support B	Support C	Support D
<b>I</b>				
Ca carbides	73	11	—	—
Fe carbides	12	34	—	—
Graphitic/aromatic carbon	7	32	74	78
C-OH groups	8	12	15	13
Carbonyl/carboxyl functionalities	—	11	11	9
$\Sigma$ C/O groups	8	23	26	22
<b>II</b>				
First reduction cycle	0.57	0.64	1.01	1.16
Second reduction cycle	0.34	0.38	0.54	0.66
Specimen	BET area ( $\text{m}^2 \text{g}^{-1}$ )		total porosity ( $\text{ml pore volume g}^{-1}$ )	
A	1095		1.39	
D	850		1.15	

*Note.* The values (I) indicate the percentage contribution to the whole measured C 1s signal region (XPS). Furthermore (II), BET surfaces and porosity values are noted and the CO adsorption values (in  $\text{ml CO g}^{-1}$ ) after impregnation with Pd (2 wt% Pd/C) are given.

nals for the aromatic/graphitic carbon were detected where the binding energy of A was 284.3 eV and that of D was 284.5 eV.

### 5. CONCLUSIONS

The physical and chemical properties of the surfaces of activated carbon supports

strongly depend on the natural carbon source and the activation procedures. XPS and SIMS data can provide information to better understand the influence of surface functional groups, aromatic/graphitic surface concentrations, and the surface hydrogen content on the precious metal dispersion

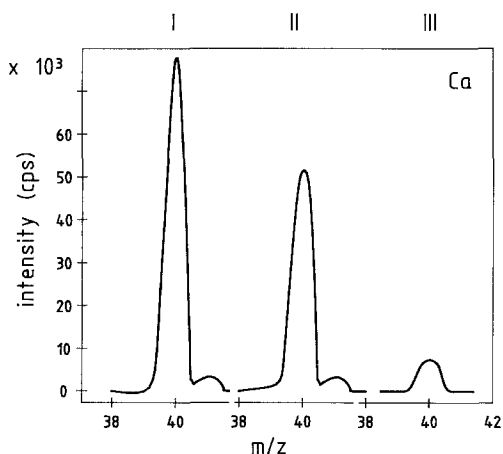


FIG. 9. Variation of the SIMS signal intensity of Ca as a function of sputtering time. (I) After 2 min. (II) After 5 min. (III) After 10 min. SIMS parameters for surface erosion: 5 keV  $\text{Ar}^+$ ,  $3 \mu\text{A cm}^{-2}$ .

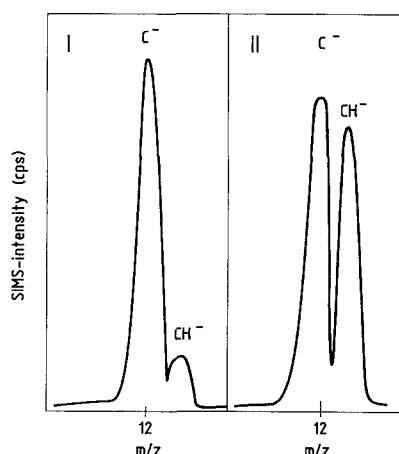


FIG. 10.  $\text{C}^-$  and  $\text{CH}^-$  fragment ions, recorded under the same SIMS conditions (see Table 4). (I) Specimen A. (II) Specimen D (enhanced  $\text{CH}^-$  intensity on support D).

and the efficiency of impregnation processes as well as the adsorption of reactants in the catalytic process.

## REFERENCES

1. Boehm, H.-P., and Knözinger, H. in "Catalysis-Science and Technology" (J. R. Anderson and M. Boudart, Ed.), p. 39, Vol. 4. Springer, Berlin, 1983.
2. von Kienle, H., and Bäder, E., "Aktivkohle und ihre industrielle Anwendung." Enke, Stuttgart, 1980.
3. Vohler, O., von Sturm, F., Wege, E., von Kienle, H., Voll, M., and Kleinschmit, P., in "Ullmann's Encyclopedia of Industrial Chemistry," Vol. A 5, p. 95. VCH, Weinheim, 1986.
4. Boehm, H. P., Diehl, E., Heck, W., and Sappok, R., *Angew. Chem.* **17**, 742 (1964).
5. Wagner, C. D., *et al.*, "Handbook of X-Ray Photoelectron Spectroscopy." Perkin-Elmer, Physical Electronics Division, Eden Prairie, MN 1978.
6. Briggs, D., and Seah, M. P., "Practical Surface Analysis by Auger and X-Ray Photoelectron Spectroscopy." Wiley, Chichester, 1985.
7. Clark, D. T., in "Handbook of X-Ray and Ultraviolet Photoelectron Spectroscopy" (D. Briggs, Ed.). Heyden, London, 1977.
8. Steinhardt, R. G., Hudis, J., and Perlmann, M. L., *Phys. Rev. B* **5**, 1016 (1972).
9. Powell, C. J., *Surf. Sci.* **44**, 29 (1974).
10. Dr. Kobs, personal communication (unpublished results).